Scientific paper

Synthesis, Antibacterial and Antibiofilm Activity of New 1,2,3,5-Tetrazine Derivatives from Coupling Reactions of Diazonium Salt of 2-Amino-6-nitrobenzothiazole With Diverse Substituted 2-Aminobenzothiazole Derivatives

Joseph Tsemeugne,^{1,*} Yetiny Atuh Bah,¹ Ulrich Joel Tsopmene,² Armelle Tontsa Tsamo,¹ Jérôme Ndefo Ndefongang,¹ Pierre Mkounga,¹ Emmanuel Fondjo Sopbué,^{3,*} Jean Paul Dzoyem,² and Augustin Ephrem Nkengfack¹

¹ Laboratory of Natural Products and Applied Organic Synthesis (LANAPOS), Department of Organic Chemistry, Faculty of Science, University of Yaounde I, P.O. Box 812, Yaounde, Republic of Cameroon;

² Laboratory of Microbiology and Antimicrobial Substances, Department of Biochemistry, Faculty of Science, University of Dschang, P.O. Box 67, Dschang, Republic of Cameroon;

³ Laboratory of Applied Synthetic Organic Chemistry, Department of Chemistry, Faculty of Science, University of Dschang, P.O. Box 67, Dschang, Republic of Cameroon

* Corresponding author: E-mail: tsemeugne@yahoo.fr, sopbue@yahoo.fr

Received: 11-12-2023

Abstract

The coupling reaction of diazonium ion of 2-amino-6-nitrobenzothiazole at 0–5 °C with distinctly substituted 2-amino-benzothiazole derivatives produced new 1,2,3,5-tetrazine derivatives. It was found that diazotized 2-amino-6-nitrobenzo[d]thiazol reacts with the ring nitrogen atom of variously substituted 2-aminobenzothiazole derivatives to yield tetrazine nucleus. The benzene ring of benzothiazole bearing electron donor group and annulated to the tetrazine was further substituted in situ by other (6-nitrobenzo[d]thiazol-2-yl)diazinyl to yield the final product. The structure of the prepared compounds was elucidated using their physical data, elemental analyses, and spectroscopic data. The synthesized compounds were tested for their antimicrobial and antibiofilm activities against Staphylococcus aureus and Escherichia coli bacteria. Two of the synthesis tetrazine derivatives exhibited interesting antibiofilm potential.

Keywords: 1,2,3,5-tetrazine, 2-aminobenzothiazole, azo dye, antibiofilm activity, antibacterial activity

1. Introduction

Tetrazine is one of the most renowned and efficient pharmaceutical class of compounds. 1,2 Tetrazines are frequently labelled in terms of their biological activities, such as possessing antibacterial, 3,4 antifungal, 5,6 anti-cancer 7,8 properties and some of them are currently used in commercially accessible products. 9 The thermal decomposition of tetrazine leads to the opening of the ring, which results in the formation of nitriles and nitrogen molecules. That is why tetrazines are also used in material sciences to make high-density energy compounds. 10–12 A wide range of methods for the synthesis of tetrazines can be found in the literature. 13 Searching for the best synthetic methodol-

ogy, we decided to use the coupling reaction of diazonium ion of 2-aminobenzothiazole with other 2-aminobenzothiazole derivatives since a similar approach was recently applied successfully in the preparation of analogous systems containing 1,2,3,5-tetrazine framework. A synthetic pathway designed in such a manner would confirm the versatility of the applied methodology. Tetrazine has three isomeric structures: 1,2,3,4-tetrazine, 1,2,3,5-tetrazine and 1,2,4,5-tetrazine, among which, 1,2,3,5-tetrazine and its derivatives are not often reported in the literature.

In medicinal chemistry, benzothiazole derivatives are well-known for their therapeutic applications. An appraisal of the recent literature showed that many effective antimicrobial drugs contain benzothiazole moiety within their structure. The benzothiazole ring system is above all a structural constituent of the marketable benzothiazole drug Riluzole. To

Compounds containing the azo functional group have revealed a wide range of medicinal applications including antibacterial, antifungal, antioxidant and anticancer, among others. Based on the above considerations, one can assume that hybrid molecular architectures containing 1,2,3,5-tetrazine, benzothiazole and azo moieties would likely combine the interesting features of all the components to exhibit much better biological profiles. ^{21–23}

2. Results and Discussion

2. 1. Chemistry

The *in situ* generated intermediate diazonium sulphate **2** (Scheme 1) was prepared by reacting 2-amino-6-nitrobenzothiazole (1) with nitrosylsulfuric acid at low temperature (0–5 $^{\circ}$ C).

 π^* transition of the benzene ring. The broad additional absorption band appearing around 350 nm is also due to an n $\rightarrow \pi^*$ transition.²⁴

In Table 2 are given the important IR data of compounds 4. One can notice the bands at 883 and 1334 cm⁻¹ which are due to the presence of tetrazine skeleton in the structures 4.²⁵ The bands at 1118 and 1209 cm⁻¹ result from skeletal vibrations of the 1,3-thiazole heterocycle.²⁶

Table 2. Assigned IR bands of the compounds 4

Frequency (cm ⁻¹)	Type of vibration and bond	Functional group
3065-2920	ν _{CAr-H}	benzyl
1614-1651	$\nu_{\mathrm{C=N}}$	1,3-thiazole
1514-1599	$\nu_{C=C}$	benzyl
1441-1487	$\nu_{N=N}$	azo group
1118-1209	$ u_{\text{C-S}}$	1,3-thiazole
883-1334	$\nu_{N-Ntetrazine}$	tetrazine

$$\begin{array}{c|c}
O_2N & S & NH_2 & NH_2 & O_2N & S & O_2N \\
\hline
 & N & N_2 & N_2$$

Scheme 1. Synthesis of the diazonium intermediate 2.

The newly prepared diazonium solution, was then coupled with other 2-aminobenzothiazole derivatives 3. The subsequent mixture was worked up as usual to yield tetrazine derivatives 4 (Scheme 2). The structure of the newly synthesized compounds 4a–d was elucidated by IR, UV, and NMR spectroscopy, as well as mass spectral data and elemental analysis data.

The UV–Vis absorption spectra of compound 4 were recorded in the range 270–475 nm, and the results are given in Table 1. All compounds displayed the two usual absorption bands of tetrazines: a weak absorption in the visible range centered around 450 nm due to the combined $n\rightarrow\pi^*$ transitions of the imine functionalities and a stronger one in the UV around 270 nm corresponding to the $\pi\rightarrow$

During the coupling reaction between the diazonium ion of 2-amino-6-nitrobenzothiazole (2) with 2-aminobenzothiazole (3a), it was established that no substitution reaction occurred between the two components as anticipated. Instead, the condensation product 4a was isolated from this reaction, probably from the subsequent nucleophilic addition of the heteroaromatic nitrogen atom of the benzothiazole ring as displayed in Scheme 3.

Compound **4a** was obtained as a red powder with a sharp melting point in the range 213–215 °C. The elemental analysis and the HREIMS experiments were used to establish the bruto formula as $C_{14}H_7N_5O_6S_3$, showing that the coupling product crystallized with one sulfate ion SO_4^{2-} . The HRMS showed an ion peak at m/z 437 corre-

Table 1: Absorption maxima (λ_{max} in nm) of the compounds 4 in methanol

Solvent	4a		4b		4c		4d	
	λ (nm)	$lg\epsilon_{max}$	λ (nm)	$lg\epsilon_{max}$	λ (nm)	$lg\epsilon_{max}$	λ (nm)	$lg \epsilon_{max}$
MeOH	277.9	3.85	273.8	4.45	270.4	4.41	277.0	4.15
	296.9	3.74	285.3	4.43	295.2	4.28	295.2	4.04
	343.9	3.86	297.7	4.34	335.6	4.44	300.1	4.04
	400.0	3.67	345.6	4.43	347.1	4.44	341.4	4.20
	470.1	3.98	396.7	4.29	367.4	4.41	364.5	4.20
			475.1	4.64	387.6	4.35	392.6	4.06
					442.9	4.45	465.2	4.24

Scheme 2. Reactions' sequences to compounds 4a-d

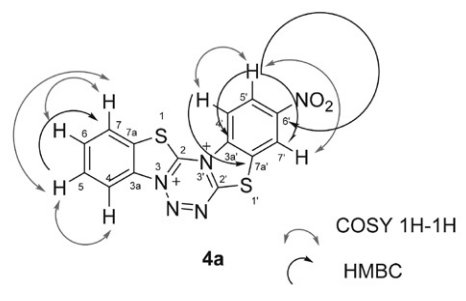
 $Scheme \ 3. \ The \ plausible \ mechanism \ for \ the \ formation \ of \ compound \ 4a.$

sponding to $[M^{+} + H]$ and characteristic fragment ion peaks at m/z: 374 $(M^{+} + H - 2S)$, 329 $(M^{+} + 2H - 2S - NO_2)$, 313 $(M^{+} + 2H - 2S - NO_2 - O)$, 285 $(M^{+} + 3H - 2S - NO_2 - O - N_2)$, 165 $(M^{+} + 2H - 2S - NO_2 - O - C_6H_4 - C_6H_2)$.

High-resolution mass spectrum reveals the surface SO_4^{2-} exchange of compounds **4a** by methanol used as a model primary alcohol for the analysis. ¹⁴ The presence on the HRMS spectrum of peaks at m/z 437 (M^{+.} – SO_4^{2-} + 3CH₃OH), 374 (M^{+.} + H⁺ + CH₃OH – SO_4^{2-}), 329 (M^{+.} + 2H⁺ + CH₃OH – SO_4^{2-} – NO_2), 263 (M^{+.} + 2H⁺ + CH₃OH – SO_4^{2-} – NO_2 – H_2S_2) proves that the sulfate of the tetrazinium salt **4a** is completely exchanged by methanol to give numerous peaks, confirming the aforementioned structural hypothesis.

The presence of the tetrazine nucleus in **4a** was further confirmed in the FTIR spectrum by the presence of the characteristic stretching bands at 1332 and 883 cm⁻¹. ²⁵ The ¹H NMR spectrum of compound **4a** gave signals at $\delta_{\rm H}$ 8.90 (d, J = 0.7 Hz, 1H, H-7'), 8.20 (d, J = 8.6 Hz, 1H, H-5'), 7.85 (d, J = 8.5 Hz, 1H, H-4') and 8.26 (d, J = 8.7 Hz, 1H,

Table 3. Important HMBC correlations in compound **4a**; 1 H and 13 C chemical shifts (δ /ppm) in DMSO- d_6 as the solvent (25 $^{\circ}$ C).



C-atom	δ ¹³ C	HMBC $(H \rightarrow C)$
7'	119.08	H -5' (8.21)
6'	155.08	H -5' (8.21)
3a'	143.87	H -4' (7.85)
2'	132.56	H -4' (7.85)
3a	127.34	H -6 (7.41)
7	123.2	H -5 (7.49)

H-4), 8.01 (d, J = 8.2 Hz, 1H, H-7), 7.49 (dd, J = 7.6 and 7.5 Hz, 1H, H-5) and 7.41 (dd, J = 7.4 and 7.6 Hz, 1H, H-6) attributable to one ABX system of nitrobenzothiazole and one ABCD system of benzothiazole $\bf 3a$, respectively. These observations confirm the proposed regio-orientation of the nucleophilic addition of the heteroaromatic N of the benzothiazole $\bf 3a$ on the diazonium ion function of $\bf 2$ instead of the electrophilic substitution on the benzene ring as initially anticipated.

The ¹³C NMR spectrum of compound **4a** shows 14 relevant signals, out of which seven [127.4, 126.0, 123.1, 122.6, 122.4, 120.9, 119.0] were assigned to the tertiary aromatic CH based on the HSQC experiments. The remaining seven signals [170.2 (C-2), 155.0 (C-6'), 144.2 (C-7a'), 143.4 (C-3a'), 132.6 (C-2'), 127.3 (C-3a), 119.6 (C-7a)] were assigned without ambiguity to the seven quaternary C-atoms thanks to the HMBC experiment (Table 3) and the comparison with simulated values.

The powder XRD spectrum of tetrazine **4a** shows many peaks which are well structured due to the good crystalline nature of compound **4a** in which atoms are organized in a regular manner.

Compound **4b** is probably formed through two-step reaction, *via* the hypothetical non isolated intermediate **4b'** over a mechanism similar to that of the formation of **4a** (Scheme 3). Favorable electronic and steric factors enable further addition of another diazonium electrophile **2** at position 7 on the electron rich benzene ring of **4b'** bearing the methyl groups (Scheme 6).

The structure of compound **4b** was elucidated by means of various spectroscopic techniques such as ¹H and ¹³C NMR spectra and elemental analysis.

Compound **4b** was obtained as a brown powder with a sharp melting point in the range 216–218 °C. The elemental analysis and the HREIMS experiments were used to establish the bruto formula as $C_{23}H_{13}N_9O_8S_4$ showing that the coupling product crystallized with one sulfate ion SO_4^{2-} .

The structure of compound **4b** is further strongly supported by its HRMS (ESI+ mode), which shows the pseudo-molecular ion peak at m/z 717 (1%) corresponding to [M⁺ + 2Na⁺] and characteristic fragment ion peaks

Scheme 6. Synthesis of compounds 4b.

Scheme 7. Some important ESI+ mode fragments of compound 4b.

at m/z 538 (1%, [M⁺ + 2Na⁺ - C₇H₃N₂O₂S]), 466 (3%, [M⁺ + 2Na⁺ + 2H - C₇H₃N₂O₂S - NO₂ - N₂]), 375 (2%, [M⁺ + 2Na⁺ + 2H - C₇H₃N₂O₂S - NO₂ - N₂ - 2S - C₂H₄]) and 181 (1%, [M⁺ + 2Na⁺ + 2H - C₇H₃N₂O₂S - NO₂ - N₂ - 2S - C₂H₄ - 2Na⁺ - 2C₆H₃]) and were assigned as shown in Scheme 7, confirming the above structural hypothesis.

The infrared spectrum of compound 4b showed absorption bands due to the stretching vibrations of the aromatic C-H at 2920 cm⁻¹, while those of N=N appeared at 1444 cm⁻¹. Two other bands belonging to the tetrazine group appear at 1334 and 881 cm⁻¹. ²⁵ The structure of synthesized tetrazine was determined based on the ¹H and ¹³C NMR chemical shifts and on the proton-proton coupling constants. On the ¹H NMR spectrum, the methyl protons on the benzothiazole ring resonated at δ_H 2.53 and 2.32 ppm, respectively as singlets.¹⁴ In the aromatic region, two ABX proton systems are exhibited at 8.88 (poorly resolved d, 1H, H-7"), 8.21 (dd, J = 8.8 and 2.2 Hz, 1H, H-5"), 7.84 (d, J = 8.8 Hz, 1H, H-4") and 8.42 (dd, J = 8.4 and 2.3 Hz,1H, H-5'), 8.28 (d, I = 9.0 Hz, 1H, H-4'), 7.96 (poorly resolved d, 1H, H-7') and a singlet at 7.76 (s, 1H, H-4) confirming the proposed regio-orientation of the electrophilic substitution of the benzothiazole diazonium ion at position 7 in the 2-amino-5,6-dimethylbenzothiazole reagent.

The 13 C NMR spectrum of the tetrazine **4b** shows 23 signals attributable to the 23 carbon atoms of the molecule. In addition, the characteristic signals of two methyl groups (CH₃) appearing at δ 20.2 and 20.1 ppm, are in agreement with the presence of a 5,6-dimethylbenzothiazole unit in the assigned structure of **4b**.

The structures of compounds **4c** and **4d** were assigned based on their analytical and spectral data by following similar reasoning as above.

The investigation into the thermal stability of tetrazine derivatives reveals that, in most instances, their stability primarily hinges on the decomposition of the substituent they carry, rather than the tetrazine ring itself.²⁷ Consequently, a subsequent examination will delve into the impact of various substituents present in compounds 4 on their stability. It is worth noting that combining two heterocyclic systems, such as benzothiazole and tetrazine as observed in compounds 4, may lead to enhanced molecular stability.²⁸ Conversely, the literature suggests that tetrazine energetic materials with limited or no oxygen content tend to yield high enthalpy species during combustion, thereby impeding the complete release of stored energy.²⁷ To address this, active oxygen can be introduced into the molecule by synthesizing tetrazine salts using inorganic oxidizing acids.²⁹ Compounds 4, crystallizing in salt form with sulphate ions as counter ions and featuring the oxygen-rich nitro function in the cationic component, could play a pivotal role in achieving complete energy release from the material. Furthermore, optimal energy performance could be attained by bringing together the endothermic cycle of tetrazine and active oxygen within the cationic segment of compounds 4.27

2. 2 Antibacterial and Antibiofilm Activity

S. aureus and E. coli are among the most frequent causes of biofilm-associated infections. With the emer-

Table 4. MIC and MBC values of the synthesized compounds and the reference antibiotic against Staphylococcus aureus and *Escherichia coli* strains.

Compounds	S. aureus ATCC1026			E. coli ATCC 10536		
	MIC	MBC	MBC/MIC	MIC	MBC	MBC/MIC
1	512	1024	2	512	>1024	_
3a	512	1024	2	1024	>1024	_
3b	1024	1024	1	1024	>1024	_
3c	1024	1024	1	1024	>1024	_
3d	512	1024	2	1024	>1024	_
4a	512	512	1	512	1024	2
4b	256	1024	2	512	>1024	_
4c	512	512	1	256	1024	4
4d	512	512	1	256	1024	4
Gentamicin 2	2	4	2	4	8	

-: not determined.

gence of antibiotic-resistancy, there is an urgent need to discover novel inhibitory compounds against these clinically important pathogens. In this study, newly synthesized 1,2,3,5-tetrazine were tested for antibacterial and antibiofilm activity against *S. aureus* and *E. coli* strains.

The antibacterial effect of the synthesized compounds and reference antibiotic gentamicin against the two bacterial strains tested, is presented in Table 4. The MIC values range from 256 µg/mL to 1024 µg/mL for tested compounds and were 2 µg/mL and 4 µg/mL for gentamicin, respectively, against *S. aureus* and *E. coli*. The results indicate that the tested compounds had moderate to weak antibacterial activity. Even though previous studies reported the activity of some tetrazine derivatives against bacterial strains, this was not the case in this study.³⁰ A plausible explanation to our findings is that the antibacterial activity of compounds might result from the basic skeleton of the molecules as well as from their nature, the number of nitrogen and sulfur atoms, and the presence of

Table 5. Percentage of the inhibition of biofilm formation (%) and the minimum biofilm inhibitory concentration (MBIC₅₀) values of the synthesized compounds against *S. aureus* and *E. coli* strains.

Compoun	ds S. aur	E. coli		
	Inhibition (%)	MBIC_{50}	Inhibition (%)	MBIC_{50}
1	34.87	_	51.68	256
3a	41.09	_	48.18	_
3b	11.54	_	14.47	_
3c	20.12	_	29.22	_
3d	71.76	128	62.45	256
4a	32.87	_	52.78	256
4b	85.53	64	64.34	128
4c	31.22	_	71.14	128
4d	34.56	_	74.83	64
Gentamici	in 83.66	8	79.21	16

—: not determined.

 NO_2 substituents.³¹ Similarly to the bactericidal nature of the reference antibiotic gentamicin, all the tested compounds showed also bactericidal activity with MBC/MBIC ratio ≤ 4 .

The result of the antibiofilm activity of the synthesized compounds and reference antibiotic gentamicin against *S. aureus* and *E. coli* strains is presented in Table 5, revealing that all the compounds showed the ability to inhibit biofilm formation to various extents. The percentage of biofilm formation inhibition varied from 11.54% to 85.53% in S. aureus and from 14.47% to 74.83% in E. coli. Compounds 1, 3d, 4a, 4b, 4c, and 4d showed more than 50% of inhibition against E. coli and two compounds (3d and 4b) against S. aureus. Compound 4b had the highest percentage of inhibition (85.53%) and MBIC₅₀ value of 64 μg/mL against S. aureus, while compound 4d showed the highest percentage of inhibition against S. aureus (74.83%) and MBIC₅₀ value of 128 μg/mL. Compounds 4b and 4d showed the lowest MBIC₅₀ value (64 μg/mL) for S. aureus and E. coli, respectively. Although several works have reported the ability of tetrazine derivatives to inhibit the growth of bacterial pathogens, studies focusing on their capacity to interfere with the formation of biofilm in bacteria are very scarce. To the best of our knowledge, this is the first study reporting the antibiofilm potential of synthesized tetrazine derivatives.

Although no rational structure-activity correlation could be established from this study, some structural features that might have predisposed the antibacterial activity of these azo compounds can be drawn from the comparison of the chemical structures of compounds with different activity. The 2-aminobenzothiazole derivatives **3c** and **3d** are differ only in position 6 with ethoxy group in compound **3c** and methoxy group in compound **3d**. Compounds **3c** and **3d** show moderate antibacterial activity in *S. aureus* and weak antibacterial activity in *E. coli* (Table 4). This difference could be linked to the different mechanisms of action of these two compounds con-

sidering that, the main difference between the two tested bacteria is the structure of their cell wall which might change their susceptibility to the compounds. In contrast, the two reaction products obtained from these two reagents, namely compounds **4c** and **4d**, show both moderate antibacterial activity on the two microorganisms tested. The improvement in the activity of compounds **4c** and **4d** on the microorganism *E. coli* could be enlightened by the improved antibacterial profiles of the hybrid compounds due to the synergetic interactions of the primary potent pharmacophores combined in the single molecular platform.

3. Experimental Section

3. 1. Chemistry

3. 1. 1. General

A Büchi melting point apparatus was used to measure uncorrected melting points. Progress of the reaction was monitored by thin-layer chromatography and the purity of compounds was checked by TLC on Eastman Chromatogram Silica Gel Sheets (13181; 6060) with fluorescent indicators. A mixture of hexane (Hex) and ethyl acetate (EA) (4:6) was used as the mobile phase and spots were visualized by iodine vapors or irradiation with UV light (254 nm). IR spectra (KBr, cm⁻¹) were recorded with a Fourier Transform Infrared spectrometer JASCO FT/IR-4100 and a Perkin-Elmer FT-IR 2000 spectrometer. The absorption spectra of the compounds were recorded with a Beckman U-640 Spectrophotometer, using samples' solutions of concentration 5·10⁻⁵ mol·L⁻¹. Elemental analyses were determined using a Euro EA CHNSO analyser from Hekatech company, and the results were found to be in good agreement ($\pm 0.3\%$) with the calculated values. Positive ion electrospray mass spectra were recorded on a 6200 series TOF/6500 series Q-TOF (11.0.221.1) mass spectrometry system running in ESI_pos_ACN_below1000_CD.m, 1 minute of acquired spectra were combined and centroided. ¹H NMR spectra were recorded in DMSO- d_6 with a 400 and 600 MHz spectrometer NMR Bruker Avance-III. ¹³C NMR spectra were recorded in DMSO- d_6 with a 100 and 150 MHz spectrometer NMR Bruker Avance-III. Tetramethylsilane (TMS) was used as the internal reference. Simulated ¹H and ¹³C(¹H) NMR spectra were performed http://www.nmrdb.org/ spectral simulation software.

3. 1. 2. Preparation of the Reagents and Starting Materials

All chemicals mentioned in this work were purchased from commercial sources and were used without further purification.

3. 1. 3. Preparation of Diazonium Salt Solution

Diazonium solution ${\bf 2}$ was prepared according to the reported procedure. 14

3. 1. 4. General Procedure for the Preparation of the Coupling Products 4

To a solution of 2-aminobenzothiazole derivatives 3a-d (10 mmol) in DMSO (10 mL) in a 500 mL conical flask cooled in an ice-bath at 0–5 °C was added drop wise over 1 h the previously prepared diazonium solution of 2 maintained at 0–5 °C. After stirring for 30 min, 15 mL of sodium acetate solution (10%) was added to the mixture. The pH of the mixtures was kept in the range 9–11. The crystals obtained were filtered on a Büchner funnel. The product was crystallized from methanol.

3-Nitrobenzo[4,5]thiazolo[3,2-c]benzo[4,5]thiazolo [3,2-e][1,2,3,5]tetrazine-8,14-diium Sulfate (4a). Obtained in 48% yield (1.74 g) as a red powder; m.p. 213-215 °C. UV/Vis (MeOH) λ_{max} (lg ϵ_{max}) see Table 1. IR (KBr) v_{max} /cm⁻¹ see Table 2. ¹H NMR (600 MHz, DMSO- d_6 , 25 °C, TMS) δ 8.90 (d, J = 0.7 Hz, 1H, H-7'), 8.26 (d, J = 8.7Hz, 1H, H-4), 8.20 (d, J = 8.6 Hz, 1H, H-5'), 8.01 (d, J = 8.2Hz, 1H, H-4), 7.85 (d, J = 8.5 Hz, 1H, H-4'), 7.49 (dd, J = 7.6and 7.5 Hz, 1H, H-5), 7.41 (dd, I = 7.4 and 7.6 Hz, 1H, H-6). 13 C NMR (150 MHz, DMSO- d_6) δ 170.2 (C-2), 155.0 (C-6'), 144.2 (C-7a'), 143.4 (C-3a'), 132.6 (C-2'), 127.5 (C-5), 127.2 (C-3a), 125.9 (C-6), 123.2 (C-7), 122.6 (C-4), 122.4 (C-5'), 120.9 (C-4'), 119.6 (C-7a), 119.2 (C-7'). HRMS ((+)-ESI) m/z (%) 437 (2), 374 (1), 329 (3), 314 (10), 285 (1), 263 (1), 200 (1), 162 (12). Anal. calcd. for C₁₄H₇N₅O₆S₃: C, 38.44; H, 1.61; N, 16.01; S, 21.99. Found: C, 38.43; H, 1.59; N, 16.00; S, 22.01. R_f 0.48 (Hex/EA 4:6).

10,11-Dimethyl-3-nitro-12-((6-nitrobenzo[d]thiazol-2-yl)diazenyl)benzo[4,5]thiazolo[3,2-c]benzo[4,5]thiazolo[3,2-e][1,2,3,5]tetrazine-8,14-diium Sulfate (4b). Obtained in 41% yield (2.75 g) as a brown powder; m.p. 216–218 °C. UV/Vis (MeOH) λ_{max} (lg ϵ_{max}) see Table 1. IR (KBr) v_{max} /cm⁻¹ see Table 2. ¹H NMR (600 MHz, DM-SO- d_6 , 25 °C, TMS) δ 8.88 (poorly resolved d, 1H, H-7"), 8.42 (dd, J = 8.4 and 2.3 Hz, 1H, H-5'), 8.28 (d, J = 9.0 Hz,1H, H-4'), 8.21 (dd, J = 8.8 and 2.2 Hz, 1H, H-5"); 7.96 (poorly resolved d, 1H, H-7'), 7.84 (d, J = 8.8 Hz, 1H, H-4"), 7.76 (s, 1H, H-4), 2.52, 2.33 (2×s, 6H, CH₃). ¹³C NMR (150 MHz, DMSO- d_6) δ 172.2 (C-2), 157.0 (C-2'), 147.5 (C-4), 145.1 (C-2"), 144.08 (C-6"), 143.7 (C-6'), 126.9 (C-6), 139.7 (C-7a'), 136.5 (C-7a"), 136.1 (C-3a'), 133.1 (C-5), 132.9 (C-3a"), 123.6 (C-3a), 123.1 (C-7'), 122.6 (C-7"), 122.2 (C-5'), 122.1 (C-5"), 120.9 (C-4'), 120.1 (C-4"), 119.5 (C-7), 118.8 (C-7a), 20.2 (CH₃), 20.1 (CH_3) . HRMS ((+)-ESI) m/z (%) 717 (1), 538 (1), 456 (1), 410 (1), 374 (2), 360 (3), 269 (1), 144 (3). Anal. Calcd. for: $C_{23}H_{13}N_9O_8S_4$: C, 41.13; H, 1.95; N, 18.77; S, 19.09. Found: C, 41.11; H, 1.94; N, 18.78; S, 19.10. $R_{\rm f}$ 0.30 (Hex/EA 4:6).

11-Ethoxy-3-nitro-12-((6-nitrobenzo[d]thiazol-2-yl)diazenyl)benzo[4,5]thiazolo[3,2-c]benzo[4,5]thiazolo[3,2-e][1,2,3,5] tetrazine-8,14-diium Sulfate (4c). Obtained in 43% yield (3.31 g) as a red powder; m.p. 205-207 °C. UV/Vis (MeOH) λ_{max} (lg ϵ_{max}) see Table 1. IR (KBr) v_{max} /cm⁻¹ see Table 2. ¹H NMR (600 MHz, DM-SO- d_6 , 25 °C, TMS) δ 8.87 (poorly resolved d, 1H, H-7"), 8.20 (dd, J = 8.7 and 1.0 Hz, 1H, H-5'), 7.90 (d, J = 8.7 Hz, 1H, H-7'), 7.84 (d, J = 8.8 Hz, 1H, H-4'), 7.74 (dd, J = 6.7and 1.6 Hz, 1H, H-5"), 7.55 (d, J = 8.8 Hz, 1H, H-5), 7.16 (d, J = 9.1 Hz, 1H, H-4), 7.08 (d, J = 8.8 Hz, 1H, H-4''), 4.10(s, 2H, CH₂), 1.59 (s, 3H, CH₃). ¹³C NMR (150 MHz, DM-SO-*d*₆) δ 174.0 (C-2), 157.2 (C-2'), 156.7 (C-2"), 146.2 (C-6), 145.2 (C-6"), 143.8 (C-7a), 143.3 (C-6'), 137.1 (C-7a'), 133.1 (C-7a"), 123.1 (C-7'), 122.8 (C-4), 122.1 (C-5'), 120.9 (C-4'), 119.4 (C-3a"), 118.7 (C-7"), 117.1 (C-3a'), 116.5 (C-3a), 116.2 (C-4"), 112.8 (C-7), 106.7 (C-5), 105.1 (C-5"), 64.13 (O-CH₂), 15.25 (CH₃). HRMS ((+)-ESI) m/z (%) 854 (4), 438 (3), 423 (11), 402 (17), 374 (11), 371 (7), 289 (1), 191 (10), 167 (3). Anal. Calcd. for $C_{23}H_{23}N_9O_{14}S_4$: C, 35.52; H, 2.98; N, 16.21; S, 16.49. Found: C, 35.49; H, 2.99; N, 16.18; S, 16.53. R_f 0.41 (Hex/EA 4:6).

11-Methoxy-3-nitro-10,12-bis((6-nitrobenzo[d]thiazol-2-yl)diazenyl)benzo[4,5]thiazolo[3,2-c]benzo[4,5]thiazolo[3,2-e][1,2,3,5]tetrazine-8,14-diium Sulfate (4d). Obtained in 54% yield (4.94 g) as a brown powder; m.p. 218–220 °C. UV/Vis (MeOH) λ_{max} (lg ϵ_{max}) see Table 1. IR (KBr) v_{max} /cm⁻¹ see Table 2. ¹H NMR (600 MHz, DM-SO- d_6 , 25 °C, TMS) δ 8.87 (d, J = 1.7 Hz, 1H, H-7'), 8.28 (s, 1H, H-4), 8.21 (dd, J = 8.8 and 2.2 Hz, 1H, H-5'), 7.94 (d, J $= 8.8 \text{ Hz}, 1\text{H}, \text{H}-4"), 7.75 (d, J = 2.5 \text{ Hz}, 1\text{H}, \text{H}-7""), 7.64 (d, J = 2.5 \text{Hz}, 1\text{H}, 1\text{H}-7""), 7.64 (d, J = 2.5 \text{Hz}, 1\text{H}, 1\text{H$ J = 2.4 Hz, 1H, H-7"), 7.58 (d, J = 8.8 Hz, 1H, H-4"), 7.38 (d,J = 8.9 Hz, 1H, H-4"), 7.20 (dd, J = 8.8 and 2.5 Hz, 1H, H-5"), 7.10 (dd, J = 8.8 and 2.3 Hz, 1H, H-5"), 4.11 (s, 3H, OCH₃). ¹³C NMR (150 MHz, DMSO- d_6) δ 170.1 (C-2), 158.3 (C-3"), 158.2 (C-6), 157.9 (C-2"), 157.5 (C-2'), 156.8 (C-3a'), 154.7 (C-3a"), 153.6 (C-3a"'), 150.8 (C-7a), 146.4 (C-6'), 145.4 (C-6"), 143.8 (C-6"), 143.4 (C-7), 137.4 (C-7a"), 137.1 (C-7a"), 133.0 (C-7a'), 123.2 (C-4"), 122.8 (C-4), 122.1 (C-5'), 120.9 (C-5), 119.3 (C-3a), 118.8 (C-7'), 118.3 (C-4'), 116.8 (C-5"), 116.0 (C-5"), 112.2 (C-4"), 106.2 (C-7"), 104.7 (C-7""), 56.3 (O-CH₃). HRMS ((+)-ESI) m/z(%) 827 (10), 717 (4), 522 (5), 452 (5), 410 (6), 408 (25), 387 (82), 196 (100), 152 (37). Anal. Calcd. for C₂₉H₁₇N₁₃O₁₃S₅: C, 38.03; H, 1.87; N, 19.88; S, 17.50. Found: C, 37.99; H, 1.85; N, 19.87; S, 17.48. R_f 0.32 (Hex/EA, 4:6).

3. 2. Antimicrobial Activity

3. 2. 1. Microorganisms and Culture Conditions

Two bacteria strains obtained from the American Type Culture Collection were used: *Staphylococcus aureus*

ATCC1026 and *Escherichia coli* ATCC 10536. They were maintained on Mueller Hinton agar slant at 4 °C and subcultured on fresh appropriate agar plates 24 h before antibacterial assay.

3. 2. 2. Minimum Inhibitory Concentration (MIC) and the Minimum Bactericidal Concentration (MBC) Determination

The minimum inhibitory concentration (MIC) and the minimum bactericidal concentration (MBC) of the synthesized compounds were determined by the broth microdilution method, as described by Bisso et al.³² Briefly, samples were prepared at 4096 µg/mL and serially diluted two-fold with Mueller Hinton agar (MHB) in a 96-well microplate at a volume of 100 μL. The concentration of the reference antibiotic and compounds ranged from 1024 to 8 μg/mL. Then, wells were filled with 100 μL of inoculum (1.5·106 CFU/mL) and the microplate was incubated at 37 °C. Wells containing only bacteria inoculum were used as negative control, while those containing microorganisms and standard drugs (gentamicin) were used as a positive control. After 24 h, 40 µL of iodonitrotetrazolium chloride (INT) solution (0.2 mg/mL) was added to each well and the microplate was further incubated for 30 min. Viable bacteria cells turned the yellow dye of INT to a pink colour. The lowest concentration of compound preventing the colour change medium was considered as the MIC. The MBC was determined by adding 50 µL from the wells that did not show growth after incubation for the MIC test to 150 uL of MHB. Then, the microplate was incubated at 37 °C for 48 h. The MBC was defined as the lowest concentration of compound that killed all bacteria. The MBC/MIC ratio was then calculated to determine the bactericidal (MBC/MIC \leq 4) or bacteriostatic (MBC/MIC > 4).³³

3. 2. 3. Biofilm Formation Inhibition Assay

The capacity of the synthesized compounds to inhibit the biofilm formation was determined using the microtiter plate method as previously described.³⁴ Briefly, 100 μL of compounds at half MIC concentration and reference antibiotic at 25 µg/mL were added in the wells of 96-well microtitre plates. Then 100 µL aliquots of bacterial cultures (1.5·106 CFU/mL) in Mueller Hinton broth supplemented with 2% glucose were added and incubated at 37 °C for 24 h. Following incubation, plates were washed with phosphate-buffered saline (PBS, pH 7.2) to remove the planktonic cells. The remaining cells in biofilms were fixed with methanol, then stained with 150 μL of safranin (1%), incubated for 15 min. After that, the excess safranin was removed, the dye bound to the cells was solubilized with 150 µL of ethanol (95%), and the optical density (OD) was measured at 570 nm using a microplate reader (Spectramax 190, Molecular Devices). The wells containing only MHB broth supplemented with 2% glucose without bacteria were used as blank while the untreated wells were the positive control. The percentage of biofilm inhibition was determined using the following formula:

$$\% \; Inhibition \; = [\frac{(ODControl - ODBlank) - \; (ODSample - ODBlank)}{(ODControl - ODBlank)}] \cdot 100$$

Compounds showing more than 50% inhibition were further two-fold serially diluted in MHB. The minimum biofilm inhibitory concentration (MBIC $_{50}$) was determined as the lowest concentration of compounds that reduces the biofilm biomass by 50%. All experiments were performed in triplicate.

4. Conclusion

An efficient procedure for the synthesis of new 1,2,3,5-tetrazine derivatives linker with a 1,3-benzothiazole ring has been presented. The diazotized title 2-amino-6-nitrobenzothiazole derivative 2 is a powerful electrophilic reagent as initially anticipated which is first attacked by the ring nitrogen atom of benzothiazoles used as couplers. Benzothiazole couplers with donor groups 3b-d further participate in an in situ electrophilic substitution reaction at its favourable non-substituted ring positions with another diazonium ion 2 to yield the corresponding 1,2,3,5-tetrazine hybrid compounds **4b-d**. Their structural assignment was done based on the obtained analytic and spectroscopic data. This study revealed that compounds 4b and 4d exhibited interesting antibiofilm potential and could be considered promising drug candidates for the development of therapeutic molecules to overcome biofilm-associated infections caused by *S. aureus* and *E. coli*.

Supplementary Information

UV spectra for compounds **4a–d**, ¹H and ¹³C NMR spectra for compounds **4a–d**, IR spectra for compounds **4a–d**, HRMS ESI+ mode of compounds **4a–d** and powder XRD patterns of compound **4a** are provided.

Acknowledgements

J. T. is grateful to Till Opatz and Paul Eckhardt for running the NMR and MS spectra. Additional financial supports for the work were obtained from the Cameroonian Ministry of Higher Education special research allocation.

5. References

 R. N. Butler: The structure, reactions, synthesis and uses of heterocyclic compounds. In Comprehensive Heterocyclic Chemistry; K. T. Potts (Ed.), Pregamon Press, Oxford, 1984,

- (5), pp. 791–838. **DOI:**10.1016/B978-008096519-2.00081-3
- R. N. Butler: The structure, reactions, synthesis and uses of heterocyclic compounds. In Comprehensive Heterocyclic Chemistry II; R. C. Storr (Ed.), Pregamon Press, Oxford, 1996, (4), pp. 621–678.

DOI:10.1016/B978-008096518-5.00095-2

Y. Méndez, G. De Armas, I. Pérez, T. Rojas, M. E. Valdés-Tresanco, M. Izquierdo, M. A. del Rivero, Y. M. Álvarez-Ginarte, P. A. Valiente, C. Soto, L. de León, A. V. Vasco, W. L. Scott, B. Westermann, J. González-Bacerio, D. G. Rivera, *Eur. J. Med. Chem.* 2019, 163, 481–499.

DOI:10.1016/j.ejmech.2018.11.074

- B. A. Hassan, H. N. Naser, M. Abdulridha, *Int. J. Res. Pharm. Sci.* 2019, 10, 1254–1258.
- P. A. Cano, A. Islas-Jácome, J. González-Marrero, L. Yépez-Mulia, F. Calzada, R. Gámez-Montaño, *Bioorg. Med. Chem.* 2014, 22, 1370–1376. DOI:10.1016/j.bmc.2013.12.069
- P. A. Cano, A. Islas-Jácome, Á. Rangel-Serrano, F. Anaya-Velázquez, F. Padilla-Vaca, E. Trujillo-Esquivel, P. Ponce-Noyola, A. Martínez-Richa, R. Gámez-Montaño, *Molecules*, 2015, 20, 12436–12449. DOI:10.3390/molecules200712436
- 7. L. V. Myznikov, A. Hrabalek, G. I. Koldobskii, *Chem. Heterocycl. Comp.* **2007**, 43, 1–9. **DOI:**10.1007/s10593-007-0001-5
- 8. J. Zhang, S. Wang, Y. Ba, Z. Xu, Eur. J. Med. Chem. **2019**, *178*, 341–351. **DOI**:10.1016/j.ejmech.2019.05.071
- S. Q. Wang, Y. F. Wang, Z. Xu, Eur. J. Med. Chem. 2019, 170, 225–234. DOI:10.1016/j.ejmech.2019.03.023
- T. Wang, C. Zheng, J. Yang, X. Zhang, X. Gong, M. Xia, J. Mol. Model. 2014, 20, 2261–2271.
- N. Saracoglu, *Tetrahedron*, 2007, 63, 4199–4235.
 DOI:10.1016/j.tet.2007.02.051
- 12. V. Sinditskii, V. Y. Egorshev, G. F. Rudakov, S. A. Filatov, A. V. Burzhava: High-Nitrogen Energetic Materials of 1,2,4,5-Tetrazine Family: Thermal and Combustion Behaviors. In Chemical Rocket Propulsion a Comprehensive Survey of Energetic Materials; L. T. de Luca, T. Shimada, V. P. Sinditskii, M. Calabro (Eds.), Springer International Publishing, Cham, Switzerland, 2017, Vol. 45, pp. 89–125.
 DOI:10.1007/978-3-319-27748-6_3
- G. Clavier, P. Audeber, Chem. Rev. 2010, 110, 3299–3314.
 DOI:10.1021/cr900357e
- 14. J. Tsemeugne, A. Y. Bah, J. P. Dzoyem, N. J. Ndefongang, I. M. Famuyide, J. Lyndy L. J. McGaw, P. K. Nangmo, B. M. W. Ouahouo, P. Mkounga, G. Edwards, P. F. W. Simon, A. Tsopmo, E. F. Sopbué, A. E. Nkengfack, *Arkivoc* 2022, (ix), 73–89. DOI:10.24820/ark.5550190.p011.866
- I. Argyropoulou, A. Geronikaki, P. Vicini, F. Zani, *Arkivoc* 2009, (vi), 89–102. DOI:10.3998/ark.5550190.0010.611
- 16. N. Naira, D. Gladsy, Pharm. Chem. 2012, 4, 1277–1282.
- S. K. Rangappa, R. P. Mahadeo, A. P. Siddappa, B. A. Srinivasa, Eur. J. Med. Chem. 2015, 89, 207–251.
- H. E. Gaffer, M. M. G. Fouda, M. E. Khalifa, *Molecules* 2016, 21, 122. DOI:10.3390/molecules21010122
- J. D. D. Tamokou, J. Tsemeugne, E. F. Sopbué, S. Prodipta, J. R. Kuiate, A. N. Djintchui, B. L. Sondengam, P. B. Kumar, *Pharmacologia* 2016, 7, 182–192.

- DOI:10.5567/pharmacologia.2016.182.192
- K. S. D. Djeukoua, F. E. Sopbué, J. D. D. Tamokou, J. Tsemeugne, P. F. W. Simon, A. Tsopmo, F. M. Tchieno, S. E. Ekom, C. N. Pecheu, I. K. Tonle, J.-R. Kuiate, *Arkivoc* 2019, (vi), 416–430. DOI:10.24820/ark.5550190.p010.994
- H. M. S. Kumar, L. Herrmann, S. B. Tsogoeva, *Bioorg. Med. Chem. Lett.* 2020, *30*, 127514.
 - DOI:10.1016/j.bmcl.2020.127514
- V. Ivasiv, C. Albertini, A. E. Gonçalves, M. Rossi, M. L. Bolognesi, *Curr. Top. Med. Chem.* 2019, 19, 1694–1711.
 DOI:10.2174/1568026619666190619115735
- 23. S. Sahil, S. Mishra, P. Singh, *Eur. J. Med. Chem.* **2016**, *124*, 500–536. **DOI**:10.1016/j.ejmech.2016.08.039
- S. F. Mason, J. Chem. Soc. 1959, 1240–1246.
 DOI:10.1039/JR9590001240
- R. H. Wiley Jr., C. H. Jarboe, F. N. Hayes, J. Org. Chem. 1957, 22, 835–836. DOI:10.1021/jo01358a609
- A. Tupys, J. Kalembkiewicz, Y. Yurii Ostapiuk, V. Matiichuk,
 O. Tymoshuk, E. Woźnicka, Ł. Byczyński, J. Therm. Anal. Calorim. 2017, 127, 2233–2242.
 DOI:10.1007/s10973-016-5784-0

- 27. V. P. Sinditskii, V. Y. Egorshev, G. F. Rudakov, S. A. Filatov, A. V. Burzhava: High-Nitrogen Energetic Materials of 1,2,4,5-Tetrazine Family: Thermal and Combustion Behaviors. In: Chemical Rocket Propulsion; L. De Luca, T. Shimada, V. Sinditskii, M. Calabro (Eds.), Springer Aerospace Technology, Springer, Cham, Switzerland, 2017.
 DOI:10.1007/978-3-319-27748-6_3
- A. I. Lesnikovich, O. A. Ivachkevich, S. V. Levchik, A. I. Balabanovich, P. N. Gaponik, A. A. Kulak, *Thermochim. Acta* 2002, 388, 233–251. DOI:10.1016/S0040-6031(02)00027-8
- J. H. Yi, F. Q. Zhao, B. Z. Wang, Q. Liu, C. Zhou, R. Z. Hu, Y. H. Ren, S. Y. Xu, K. Z. Xu, X. N. Ren, J. Hazard. Mater. 2010, 181(1-3), 432-443. DOI:10.1016/j.jhazmat.2010.05.029
- 30. A. A. M. El-Reedy, N. K. Soliman, Sci. Rep. 2020, 10(1), 6137.
- 31. M. A. Al-Omair, A. R. Sayed, M. M. Youssef, *Molecules* **2015**, 20(2), 2591–2610. **DOI:**10.3390/molecules20022591
- B. N. Bisso, R. N. E. Nkwele, T. R. Tchuenguem, J. P. Dzoyem, *Adv. Pharmacol. Pharm. Sci.* 2022, 1–8.
 DOI:10.1155/2022/1998808
- G. A. Pankey, L. D. Sabath, Clin. Infect. Dis. 2004, 38, 864–870. DOI:10.1086/381972
- B. N. Bisso, T. C. R. Kuaté, J. P. Dzoyem, Can. J. Infect. Dis. Med. Microbiol. 2021, 7029944.

Povzetek

Z reakcijo pripajanja diazonijevega iona 2-amino-6-nitrobenzotiazola pri 0–5 °C na substituirane derivate 2-aminobenzotiazola smo pripravili nove 1,2,3,5-tetrazinske derivate. Ugotovili smo, da diazotirani 2-amino-6-nitrobenzo[d]tiazol reagira z obročnim dušikovim atomom različno substituiranih 2-aminobenzotiazolnih derivatov; ob tem nastane tetrazinski obroč. Benzenski obroč benzotiazolov, ki vsebuje elektron donorsko skupino in je pripojen k tetrazinskemu, smo dodatno in situ substituirali z drugimi (6-nitrobenzo[d]tiazol-2-il)diazinili, da smo dobili končni produkt. Strukture pripravljenih spojin smo določili glede na njihove fizikalne lastnosti, elementno analizo in spektroskopske podatke. Pripravljenim spojinam smo določili antimikrobno aktivnost ter aktivnost proti tvorbi biofilma z bakterijama Staphylococcus aureus in Escherichia coli. Dva izmed pripravljenih tetrazinskih derivatov sta pokazala zanimiv potencial pri preprečevanju tvorbe biofilmov.



Except when otherwise noted, articles in this journal are published under the terms and conditions of the Creative Commons Attribution 4.0 International License